IOPscience iopscience.iop.org

Home Search Collections Journals About Contact us My IOPscience

Theory of polariton-mediated Raman scattering in microcavities

This article has been downloaded from IOPscience. Please scroll down to see the full text article.

2007 J. Phys.: Condens. Matter 19 176210

(http://iopscience.iop.org/0953-8984/19/17/176210)

View the table of contents for this issue, or go to the journal homepage for more

Download details:
IP Address: 129.252.86.83
The article was downloaded on 28/05/2010 at 17:53

Please note that terms and conditions apply.

IOP PUBLISHING JOURNAL OF PHYSICS: CONDENSED MATTER

J. Phys.: Condens. Matter **19** (2007) 176210 (7pp) doi:10.1088/0953-8984/19/17/176210

Theory of polariton-mediated Raman scattering in microcavities

L M León Hilario, A Bruchhausen, A M Lobos and A A Aligia

Centro Atómico Bariloche and Instituto Balseiro, Comisión Nacional de Energía Atómica, 8400 S. C. de Bariloche, Argentina

Received 28 December 2006, in final form 9 February 2007
Published 28 March 2007
Online at stacks.iop.org/JPhysCM/19/176210

Abstract

We calculate the intensity of the polariton-mediated inelastic light scattering in semiconductor microcavities. We treat the exciton–photon coupling nonperturbatively and incorporate lifetime effects in both excitons and photons, and a coupling of the photons to the electron–hole continuum. Taking the matrix elements as fitting parameters, the results are in excellent agreement with measured Raman intensities due to optical phonons that are resonant with the upper polariton branches in II–VI microcavities with embedded CdTe quantum wells.

Planar semiconductor microcavities (MCs) have attracted much attention in the last decade as they provide a novel means to study, enhance and control the interaction between light and matter [1–6]. When the MC mode (cavity photon) is tuned in near resonance with the embedded quantum well (QW) excitonic transitions, and the damping processes involved are weak in comparison to the photon–matter interaction, the eigenstates of the system become mixed exciton–photon states, *cavity polaritons*, which are in part light and in part matter bosonic quasiparticles [1–3]. Examples of interesting new physics are the recent evidence of a Bose–Einstein condensation of polaritons in CdTe MCs [4, 5], and the construction of devices which increase the interaction of sound and light, opening the possibility of realizing a coherent monochromatic source of acoustic phonons [6].

Raman scattering due to longitudinal optical (LO) phonons, being a coherent process, is intrinsically connected with the cavity polariton. The physics of strongly coupled photons and excitons, the polariton–phonon interaction, and the polariton–external-photon coupling are clearly displayed [7–11]. In particular, resonant Raman scattering (RRS) experiments, in which the wavelength of the incoming radiation is tuned in a way such that, after the emission of an LO phonon, the energy of the outgoing radiation coincides with that of the cavity polariton branches, have proven to be suited to sense the dynamics of the coupled modes, and to obtain information about the dephasing of the resonant polaritonic state [7–11]. Unfortunately, due to the large remaining luminescence, RRS experiments in resonance with the lower polariton

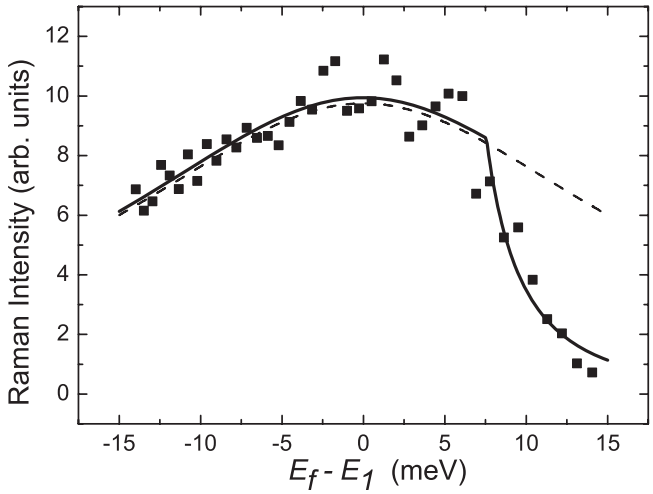

Figure 1. Raman intensity as a function of detuning for sample A. Solid squares: experimental results [9]. Solid line: theory (equation (9)) for $B - E_1 = 14$ meV, $\delta_f = \delta_1 = 0.1$ meV, and $A = 0.031$. Dashed line: result for a 2×2 matrix (equation (2)).

branch have not yet been achieved in intrinsic II–VI MCs[1]. Therefore all reported experiments in these kinds of MCs, with embedded CdTe QWs, consider the case of the scattered photons being in resonance with the upper polariton branch for two-branch systems (coupling of one exciton mode and the cavity photon) or with the middle polariton branch for three-branch systems (coupling of two exciton modes and the cavity photon) [8, 9, 12]. The measured intensities in these systems were analysed on the basis of a model in which one (or two) exciton state(s) $|e\rangle$ is (are) mixed with a photon state $|f\rangle$ with the same in-plane wavevector $\mathbf{k}$, leading to a 2×2 (3×3) matrix. Essentially, the Raman intensity is proportional to

$$I \sim T_i T_s |\langle P_i | H' | P_s \rangle|^2, \tag{1}$$

where T_i describes the probability of conversion of an incident photon $|f_i\rangle$ into the polariton state $|P_i\rangle$, T_s has an analogous meaning for the scattered polariton $|P_s\rangle$ and the outgoing photon $|f_s\rangle$, and H' is the interaction between electrons and the LO phonons. At the conditions of resonance with the outgoing polariton, T_i is very weakly dependent on the laser energy or detuning (the difference between photon and exciton energies), while T_s is proportional to the photon strength of the scattered polariton, $|\langle f_s | P_s \rangle|^2$. Similarly, in the simplest case of only one exciton (2×2 matrix) one expects that the matrix element entering equation (1) is proportional to the exciton part of the scattered polariton, $|\langle P_i | H' | P_s \rangle|^2 \sim |\langle e_s | P_s \rangle|^2$. Thus if the wavefunction is $|P_s\rangle = \alpha |f_s\rangle + \beta |e_s\rangle$, one has

$$I \sim |\langle f_s | P_s \rangle|^2 |\langle e_s | P_s \rangle|^2 = |\alpha|^2 |\beta|^2. \tag{2}$$

This model predicts a Raman intensity which is symmetric with detuning and is maximum at zero detuning. In other words, the intensity is maximum for detunings such that the scattered polariton is more easily coupled to the external photons, but at the same time when the polariton is more easily coupled to the optical phonons, which requires a large matter (exciton) component of the polariton. This result is in qualitative agreement with experiment [9]. However, for positive detuning, the experimental results fall below the values predicted by

[1] RRS experiments in resonance with the lower polariton branch have only been reported in III–VI samples with doped Bragg reflectors (see [10] and [11] for details).

equation (2) (see figure 1). This is ascribed to the effects of the electron–hole continuum above the exciton energy, which are not included in the model [9].

For another sample in which two excitons are involved, the above analysis can be extended straightforwardly and the intensity depends on the amplitudes of a 3×3 matrix and the matrix element of H' involving both excitons [9]. However, comparison with experiments at resonance with the middle polariton branch shows a poorer agreement than in the previous case (see figure 6 of [9]). In addition, a loss of coherence between the scattering of both excitons with the LO phonon was assumed, which is hard to justify. Some improvement has been obtained recently when damping effects are introduced phenomenologically as imaginary parts of the photon and exciton energies, but still a complete loss of coherence resulted from the fit [12, 13].

In this paper we include the states of the electron–hole continuum, and the damping effects in a more rigorous way. Using some matrix elements as free parameters, we can accurately describe the Raman intensities for both samples studied in [9].

In the experiments with CdTe QWs inside II–VI MCs, the light is incident perpendicular to the (x, y) plane of the QWs and is collected in the same direction z. Therefore the in-plane wavevector $\mathbf{K} = 0$, the polarization of the electric field, should lie in the (x, y) plane, and the excitons which couple with the light should have the same symmetry as the electric field (one of the two Γ_5 states of heavy hole excitons [14]). Thus, to lighten the notation we suppress the wavevector and polarization indices. The basic ingredients of the theory are two or three strongly coupled boson modes, one for the light MC eigenmode with boson creation operator $f^\dagger$, another one for the 1s exciton (e_1), and, if necessary, the 2s exciton (e_2) is also included. We assume that each of these boson states mixes with a continuum of bosonic excitations which broadens its spectral density. In addition, we include the electron–hole continuum above the exciton states, described by bosonic operators $c^\dagger_{\mathbf{k}}$, $c_{\mathbf{k}}$, where $\mathbf{k}$ is the difference between electron and hole momentum in the (x, y) plane (the sum is $\mathbf{K} = 0$ because it is conserved).

The Hamiltonian reads

$$H = E_f f^\dagger f + \sum_i E_i e_i^\dagger e_i + \sum_i (V_i e_i^\dagger f + \text{H.c.}) + \sum_p \epsilon_p r_p^\dagger r_p + \sum_p (V_p r_p^\dagger f + \text{H.c.}) + \sum_{i\mathbf{q}} \epsilon_{i\mathbf{q}} d_{i\mathbf{q}}^\dagger d_{i\mathbf{q}} + \sum_{i\mathbf{q}} (V_{i\mathbf{q}} d_{i\mathbf{q}}^\dagger e_i + \text{H.c.}) + \sum_{\mathbf{k}} \epsilon_{\mathbf{k}} c_{\mathbf{k}}^\dagger c_{\mathbf{k}} + \sum_{\mathbf{k}} (V_{\mathbf{k}} c_{\mathbf{k}}^\dagger f + \text{H.c.}). \tag{3}$$

The first three terms describe the strong coupling between the MC photon and the exciton(s) already included in previous approaches [9, 13]. The fourth and fifth terms describe a continuum of radiative modes and its coupling to the MC light eigenmode. Their main effect is to broaden the spectral density of the latter even in the absence of light–matter interaction. The following two terms have a similar effect for the exciton mode(s). The detailed structure of the states described by the $d^\dagger_{i\mathbf{q}}$ operators is not important in what follows. They might describe combined excitations due to scattering with acoustical phonons. The last two terms correspond to the energy of the electron–hole excitations and their coupling to the MC light mode.

In equation (3), we make the usual approximation of neglecting the internal fermionic structure of the excitons and electron–hole operators and taking them as free bosons. This is an excellent approximation for the conditions of the experiment. We also neglect terms which do not conserve the number of bosons. Their effect is small for the energies of interest [15]. These approximations allow us formally to diagonalize the Hamiltonian by a Bogoliubov transformation. The diagonalized Hamiltonian has the form $H = \sum_\nu E_\nu p_\nu^\dagger p_\nu$, where the boson operators $p_\nu^\dagger$ correspond to generalized polariton operators and are linear combinations of all creation operators entering equation (3). Denoting the latter for brevity as $b_j^\dagger$, then $p_\nu^\dagger = \sum_j A_{\nu j} b_j^\dagger$. In practice, instead of calculating the E_ν and $A_{\nu j}$, it is more convenient to

work with the retarded Green's functions $G_{jl}(\omega) = \langle\langle b_j; b_l^\dagger\rangle\rangle_\omega$ and their equations of motion

$$\omega\langle\langle b_j; b_l^\dagger\rangle\rangle_\omega = \delta_{jl} + \langle\langle [b_j, H]; b_l^\dagger\rangle\rangle_\omega. \tag{4}$$

As we show below, the RRS intensity can be expressed in terms of spectral densities derived from these Green's functions, which in turn can be calculated using equation (4).

Using Fermi's golden rule, the probability per unit time for a transition from a polariton state $|i\rangle = p_{\nu'}^\dagger|0\rangle$ to states $|s\rangle = p_\nu^\dagger a^\dagger|0\rangle$, where $a^\dagger$ creates an LO phonon, is

$$W = \frac{2\pi}{\hbar}|\langle i|H'|s\rangle|^2\rho(\omega), \qquad \text{where } \rho(\omega) = \sum_\nu \delta(\omega - E_\nu) = -\frac{1}{\pi}\mathrm{Im}G_{\nu\nu}(\omega + \mathrm{i}0^+) \tag{5}$$

is the density of final states. As argued above, we neglect the dependence of T_i on frequency and take $T_s = |A_{\nu f}|^2$, the weight of photons in the scattered eigenstates. In addition, H' should be proportional to the matter (exciton) part of the scattered polariton states. Then, the Raman intensity is proportional to

$$WT_s \propto I = |A_{\nu e1} + \alpha A_{\nu e2}|^2|A_{\nu f}|^2\rho(\omega). \tag{6}$$

Here we are neglecting the contribution of the electron–hole continuum to H', and α is the ratio of matrix elements of the exciton–LO phonon interaction between 2s and 1s excitons. If the 2s excitons are unimportant, $\alpha = 0$.

Using equations (4) it can be shown that

$$\rho_{jl}(\omega) = -\frac{1}{2\pi}[G_{jl}(\omega + \mathrm{i}0^+) - G_{jl}(\omega - \mathrm{i}0^-)] = A_{\nu j}\bar{A}_{\nu l}\rho(\omega). \tag{7}$$

From here and $\sum_j |A_{\nu j}|^2 = 1$, it follows that $\rho(\omega) = \sum_j \rho_{jj}(\omega)$. Replacing in equation (6) we obtain

$$I(\omega) = \frac{\rho_{ff}[\rho_{e1,e1} + |\alpha|^2\rho_{e2,e2} + 2\mathrm{Re}(\alpha\rho_{e2,e1})]}{\sum_j \rho_{jj}(\omega)}. \tag{8}$$

In practice, when ω is chosen such that the resonance condition for the outgoing polariton is fulfilled, we can neglect the contribution of the continuum states in the denominator of equation (8). In particular, if the contribution of the 2s exciton can be neglected (as in sample A of [9]),

$$I(\omega) = \frac{\rho_{ff}(\omega)\rho_{e1,e1}(\omega)}{\rho_{ff}(\omega) + \rho_{e1,e1}(\omega)}. \tag{9}$$

The Green's functions are calculated from the equations of motion (4). In the final expressions, the continuum states enter through the following sums:

$$S_f(\omega) = \sum_p \frac{|V_p|^2}{\omega + \mathrm{i}0^+ - \epsilon_p}, \quad S_i(\omega) = \sum_{\mathbf{q}} \frac{|V_{i\mathbf{q}}|^2}{\omega + \mathrm{i}0^+ - \epsilon_{i\mathbf{q}}}, \quad S'_f(\omega) = \sum_{\mathbf{k}} \frac{|V_{\mathbf{k}}|^2}{\omega + \mathrm{i}0^+ - \epsilon_{\mathbf{k}}}. \tag{10}$$

For the first two we assume that the results are imaginary constants that we take as parameters:

$$S_f(\omega) = -\mathrm{i}\delta_f, \qquad S_j(\omega) = -\mathrm{i}\delta_j. \tag{11}$$

This is the result expected for constant density of states and matrix elements. Our results seem to indicate that this assumption is valid for the upper and middle polariton branches. For the lower branch at small $\mathbf{k}$, it has been shown that the line width due to the interaction of polaritons with acoustic phonons depends on the detuning $E_f - E_1$ and $k_\parallel$, being smaller for small wavevector [16, 17].

The electron–hole continuum begins at the energy of the gap and corresponds to vertical transitions in which the light promotes a valence electron with two-dimensional wavevector $\mathbf{k}$ to the conduction band with the same wavevector. In the effective-mass approximation, the energy is quadratic with $\mathbf{k}$, and this leads to a constant density of states beginning at the gap. The matrix element $V_{\mathbf{k}}$ is proportional to $M_{\mathbf{k}} = \langle \mathbf{k}_v | p_E | \mathbf{k}_c \rangle$, where p_E is the momentum operator in the direction of the electric field, and $|\mathbf{k}_v\rangle$, $|\mathbf{k}_c\rangle$ are the wavefunctions for valence and conduction electrons with wavevector $\mathbf{k}$. Taking these wavefunctions as plane waves, one has $M_{\mathbf{k}} \sim k_E$, the wavevector in the direction of the electric field. Then $|V_{\mathbf{k}}|^2 \sim k_E^2$. Adding the contributions of all directions of $\mathbf{k}$ one has $|V_{\mathbf{k}}|^2 \sim |\mathbf{k}|^2 \sim \epsilon_{\mathbf{k}}$ (linear with energy for small energy). This leads to

$$S'_f = R(\omega) - \mathrm{i}A(\omega - B)\Theta(\omega - B), \tag{12}$$

where B is the bottom of the electron–hole continuum (the energy of the semiconductor gap) and A is a dimensionless parameter that controls the magnitude of the interaction. The real part $R(\omega)$ can be absorbed in a renormalization of the photon energy and is unimportant in what follows. The imaginary part is a correction to the photon width for energies above the bottom of the continuum.

Using the theory outlined above, we calculated the intensity of RRS corresponding to the samples A and B measured in [9, 12] and compared them with the experimental results.

Sample A corresponds to the simplest case. Two polariton branches are seen and therefore only the 1s exciton plays a significant role. The binding energy of this exciton $B - E_1$ is not well known. The Rabi splitting $2V_1 = 19$ meV. The width of the Raman scan as a function of frequency for zero detuning is of the order of $w = 0.1$ meV (see figure 3 of [9]). This implies the relation $2w^2 = \delta_f^2 + \delta_1^2$ in our theory. In any case, the results are weakly sensitive to w. Therefore, we have three free parameters in our theory in addition to a multiplicative constant: $B - E_1$, the ratio of widths δ_f/δ_1 and the slope A.

The comparison between the experimental and the theoretical intensities is shown in figure 1 for a set of parameters that lead to a close agreement with experiment. The condition of resonance is established by choosing the energy ω for which the intensity given by equation (9) has its second relative maximum (corresponding to the upper polariton branch). The dashed line corresponds to the case in which only the first three terms (with $i = 1$) in the Hamiltonian, equation (3), are included. In this case, the intensity is given in terms of the solution of a 2×2 matrix (equation (2)) and was used in [9] to interpret the data. This simple expression gives a Raman intensity which is an even function of the detuning. When the full model is considered, the Raman intensity falls more rapidly for large detuning $E_f - E_1$ as a consequence of the hybridization of the photon with the electron–hole continuum. When the energy of the polariton increases beyond B entering the electron–hole continuum (corresponding to the kink in figure 1), the Raman peak broadens and loses intensity. The kink can be smoothed if the effect of the infinite excitonic levels below the continuum is included in the model (leading to an S'_f with continuous first derivative), but this is beyond the scope of this work. If the ratio δ_f/δ_1 is enlarged, the Raman intensity increases for negative detuning with respect to its value for positive detuning.

In the experiments with sample B three polariton branches are observed [12], and the 2s exciton plays a role. Experimentally, it is known that the binding energy for the two excitons are $B - E_1 = 17$ meV and $B - E_2 = 2$ meV. From the observed Rabi splitting one has $2V_1 = 13$ meV, $2V_2 = 2.5$ meV. In comparison with the previous case, we have the additional parameter α (the ratio of exciton–LO phonon matrix elements). In addition, to be able to describe well the intensity for low energies of the middle polariton (left part of the curve shown in figure 2), we need to assume a small linear dependence of E_1 with the position of the incident

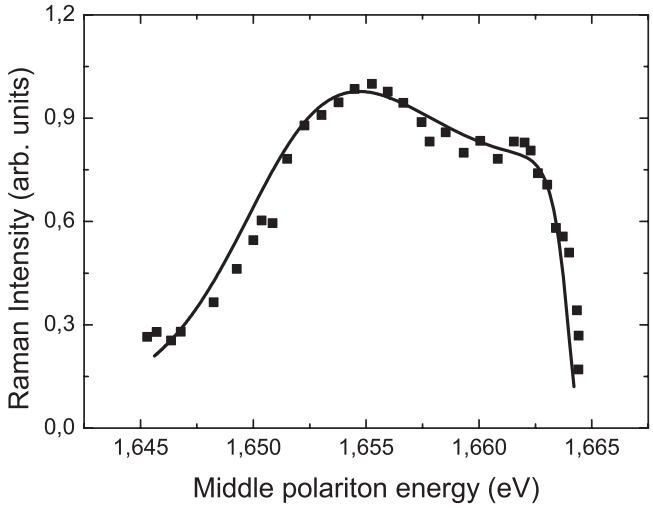

Figure 2. Raman intensity as a function of the middle polariton energy. Solid squares: experimental results [12]. Solid line: theory for $\delta_f = 0.2$, $\delta_1 = 0.1$, $\delta_2 = 0.12$, $\alpha = -0.45$ and $z = 0.14$. A is the same as in figure 1.

laser spot in the sample. This dependence is also inferred from the observed luminescence spectrum [12]. In our model, this corresponds to a dependence of E_1 on E_f:

$$E_1 = E_1^0 + z(E_f - E_1^0). \tag{13}$$

In figure 2 we show the intensity at the second maximum of $I(\omega)$ (corresponding to the middle polariton branch) as a function of the energy of this maximum. We also show in the figure experimental results taken at lower laser excitation and a slightly higher temperature (4.5 K) than those reported in [9].

The slope which better describes the data is $z = 0.14$. This value is close to $z = 0.155$ which was obtained from a fit of the maxima of luminescence spectrum of the lower and middle polaritons. We have taken the same value for A as in figure 1. The agreement between theory and experiment is remarkable. As for sample A, the values of δ_i that result from the fit are reasonable in comparison with calculated values [16].

In summary, we have proposed a theory to calculate the Raman intensity for excitation of longitudinal optical phonons in microcavities, in which different matrix elements are incorporated as parameters of the model. The most important advance in comparison with previous simplified theories [9, 13] is the inclusion of the strong coupling of the electron–hole continuum with the microcavity photon. Inclusion of this coupling is essential when the energy of the polariton is near the bottom of the conduction band (at the right of figure 1). We have also included the effects of damping of excitons and photons, coupling them with a continuum of bosonic excitations. Simpler approaches have included the spectral widths δ_f and δ_i of photons and excitons as imaginary parts of the respective energies, leading to non-Hermitian matrices.

Taking some of the parameters of the model as free (δ_f/δ_i, $B - E_1$ and A for sample A, δ_f, δ_i, z and α for sample B), we obtain excellent fits of the observed Raman intensities. The resulting values of the parameters agree with previous estimates, if they are available. We are not aware of previous estimates for A and α. As an important improvement to previous approaches [9, 13] for the case of sample B, we do not have to assume a partial loss of coherence between 1s and 2s excitons in their scattering with the LO phonon.

Further progress in the understanding of the interaction of excitons with light and phonons requires microscopic calculations of the parameters δ_f, δ_i, A and α, and the effects of the temperature on them. However, taking into account the difficulties in calculating these parameters accurately, the present results are encouraging and suggest that the main physical ingredients are included in our model.

Acknowledgments

We thank A Fainstein for useful discussions. This work was supported by PIP 5254 of CONICET and PICT 03-13829 of ANPCyT.

References

[1] Kavokin A and Malpuech G 2003 *Cavity Polaritons* (Amsterdam: Elsevier)
[2] 2003 Microcavities *Semicond. Sci. Technol.* **18** S279–434 (Special issue)
[3] 2006 Photon-mediated phenomena in semiconductor nanostructures *J. Phys.: Condens. Matter* **18** S3549–768 (Special issue)
[4] Kasprzak J, Richard M, Kundermann M, Baas A, Jeambrun P, Keeling J M J, Marchetti F M, Szymanska M H, André R, Staehli J L, Savona V, Littlewood P B, Deveaud B and Le S D 2006 *Nature* **443** 409
[5] Deng H, Press D, Götzinger S, Solomon G S, Hey R, Ploog K H and Yamamoto Y 2006 *Phys. Rev. Lett.* **97** 146402
[6] Trigo M, Bruchhausen A, Fainstein A, Jusserand B and Thierry-Mieg V 2002 *Phys. Rev. Lett.* **89** 227402
[7] Fainstein A, Jusserand B and Thierry-Mieg V 1997 *Phys. Rev. Lett.* **78** 1576
[8] Fainstein A, Jusserand B and André R 1998 *Phys. Rev.* B **57** R9439
[9] Bruchhausen A, Fainstein A, Jusserand B and André R 2003 *Phys. Rev.* B **68** 205326
[10] Tribe W R, Baxter D, Skolnick M S, Mowbray D J, Fisher T A and Roberts J S 1997 *Phys. Rev.* B **56** 12429
[11] Stevenson R M, Astratov V N, Skolnick M S, Roberts J S and Hill G 2003 *Phys. Rev.* B **67** 081301(R)
[12] Fainstein A and Jusserand B 2006 *Light Scattering in Solids* vol 9, ed M Cardona and R Merlin (Berlin: Springer)
[13] Bruchhausen A, Fainstein A and Jusserand B 2005 *Physics of Semiconductors CP772* ed J Menéndez and C G Van de Walle (New York: AIP) p 1117
[14] Jorda S, Rössler U and Broido D 1993 *Phys. Rev.* B **48** 1669
[15] Jorda S 1994 *Phys. Rev.* B **50** 2283
[16] Savona V and Piermarocchi C 1997 *Phys. Status Solidi* a **164** 45
[17] Cassabois G, Triques A L C, Bogani F, Delalande C, Roussignol Ph and Piermarocchi C 2000 *Phys. Rev.* B **61** 1696